Solid State Nuclear Magnetic Resonance 111 (2021) 101701

Contents lists available at ScienceDirect

Solid State Nuclear Magnetic Resonance

journal homepage: www.elsevier.com/locate/ssnmr

$^{1}H/^{13}C/^{15}N$ triple-resonance experiments for structure determinaton of membrane proteins by oriented-sample NMR

Joel Lapin, Emmanuel O. Awosanya, Richard J.A. Esteves, Alexander A. Nevzorov *

Department of Chemistry, North Carolina State University, 2620 Yarbrough Drive, Raleigh, NC, 27695-8204 USA

ARTICLE INFO

Keywords:
NMR pulse sequence design
Triple-resonance experiments
Dipolar couplings
Separated local-field spectroscopy
ROULETTE
Membrane proteins
Structure determination
Heteronuclear correlations

ABSTRACT

The benefits of triple-resonance experiments for structure determination of macroscopically oriented membrane proteins by solid-state NMR are discussed. While double-resonance $^{1}H/^{15}N$ experiments are effective for structure elucidation of alpha-helical domains, extension of the method of oriented samples to more complex topologies and assessing side-chain conformations necessitates further development of triple-resonance ($^{1}H/^{13}C/^{15}N$) NMR pulse sequences. Incorporating additional spectroscopic dimensions involving ^{13}C spin-bearing nuclei, however, introduces essential complications arising from the wide frequency range of the ^{1}H-^{13}C dipolar couplings and ^{13}C CSA (>20 kHz), and the presence of the ^{13}C-^{13}C homonuclear dipole-dipole interactions. The recently reported ROULETTE–CAHA pulse sequence, in combination with the selective z-filtering, can be used to evolve the structurally informative ^{1}H-^{13}C dipolar coupling arising from the aliphatic carbons while suppressing the signals from the carbonyl and methyl regions. Proton-mediated magnetization transfer under mismatched Hartman-Hahn conditions (MMHH) can be used to correlate ^{13}C and ^{15}N nuclei in such triple-resonance experiments for the subsequent ^{15}N detection. The recently developed pulse sequences are illustrated for n-acetyl Leucine (NAL) single crystal and doubly labeled Pf1 coat protein reconstituted in magnetically aligned bicelles. An interesting observation is that in the case of ^{15}N-labeled NAL measured at ^{13}C natural abundance, the triple ($^{1}H/^{13}C/^{15}N$) MMHH scheme predominantly gives rise to long-range intermolecular magnetization transfers from ^{13}C to ^{15}N spins; whereas direct Hartmann-Hahn $^{13}C/^{15}N$ transfer is entirely intramolecular. The presented developments advance NMR of oriented samples for structure determination of membrane proteins and liquid crystals.

1. Introduction

Solid-state NMR is a powerful, minimally invasive technique for structure elucidation of membrane proteins in their near-native lipid environments. Oriented-sample (OS) NMR serves as a complementary technique to magic-angle spinning (MAS) NMR by providing angular-dependent experimental restraints for structure determination of uniaxially aligned membrane proteins. Moreover, OS NMR allows one to study membrane proteins in planar, lipid rich bilayers at high lipid-to-protein ratios. Macroscopic alignment of the sample with respect to the magnetic field can be achieved in OS NMR by either mechanical or magnetic methods. As an example of mechanical alignment, glass plates have been successfully utilized for structure determination of membrane proteins over many years [1–11]. Alternatively, bicellar bilayers or bicelles [12–17] spontaneously align in high magnetic fields, thus providing an oriented membrane mimetic for structure-function studies of membrane proteins. The natural magnetic alignment state for bicelles corresponds to their membrane normal being perpendicular to the main magnetic field due to the negative sign of the magnetic susceptibility anisotropy of the lipid hydrocarbon interior [18]. The parallel alignment as in glass plates can be achieved for bicelles by either adding lanthanide ions [17,19,20] or by replacing DMPC lipids with biphenyl lipids [21], which make the bilayer susceptibility anisotropy positive. Very recently, magnetically oriented macrodiscs [22–25] have been introduced in OS NMR exhibiting exceptional linewidths [24] due to the high degree of alignment.

It is important to note, however, that in most if not all of the above examples of structure determination of membrane proteins by OS NMR only double resonance ($^{1}H/^{15}N$) NMR experiments have been utilized. Typically, a protein structure is calculated by combining the ^{15}N chemical shift anisotropy (CSA) with ^{1}H-^{15}N dipolar couplings (DCs) obtained from high-resolution separated local-field (SLF) experiments such as PISEMA [26], HIMSELF [27] and SAMPI4 [28]. These angular-dependent restraints are used to determine the possible orientations of the peptide

* Corresponding author.
E-mail address: alex_nevzorov@ncsu.edu (A.A. Nevzorov).

https://doi.org/10.1016/j.ssnmr.2020.101701
Received 14 September 2020; Accepted 13 November 2020
Available online 24 November 2020

planes and subsequently the possible combinations of the torsion angles Φ and Ψ between them [29,30]. However, due to the even parity of the of the ^{15}N CSA and ^{1}H-^{15}N dipolar interactions, as well as the relative orientations of their tensors having two principal axes within the same peptide plane, multiple orientational solutions can be consistent with a given set of two-dimensional experimental NMR data. This geometric ambiguity necessitates invoking *a priori* assumptions about the secondary structure(s) of a membrane protein. As a result, double resonance OS NMR experiments are most effective for calculating structures of relatively short alpha helices.

^{13}C NMR has been widely utilized in solution and MAS NMR for obtaining spectroscopic assignments and distance information. The

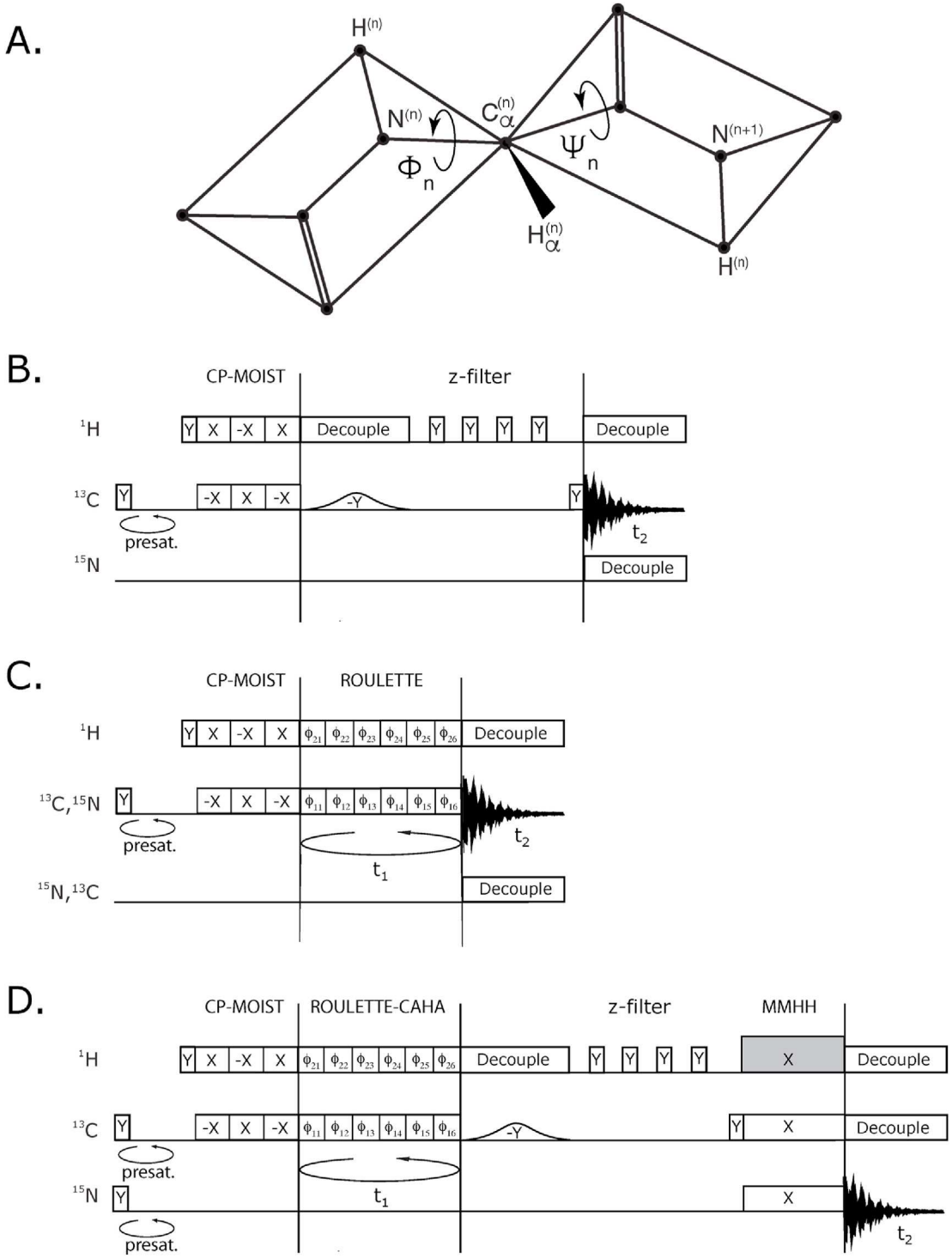

Fig. 1. A. Structure determination of oriented membrane proteins by OS NMR involves the measurements of angular-dependent restraints such as ^{1}H-^{15}N dipolar couplings and ^{15}N CSA for two adjacent peptide planes, n and n+1, from which the linking torsion angles Φ_n and Ψ_n can be determined. Incorporation of additional chiral $C_\alpha H_\alpha$ couplings greatly reduces the number of the possible (Φ_n, Ψ_n) pair solutions. B. 1D Selective excitation sequence where the aliphatic region is selected by a Gaussian pulse followed by a z-filter incorporating a few saturating pulses on the ^{1}H channel. C. ROULETTE-type SLF sequence for measuring ^{13}C-detected ^{1}H-^{13}C couplings or ^{15}N detected ^{1}H-^{15}N couplings. D. Triple-resonance 2D PS for measuring ^{15}N-detected ^{1}H-^{13}C couplings. ^{1}H-^{13}C dipolar couplings are evolved by the ROULETTE-CAHA sequence, whereas the ^{13}C/^{15}N correlations are achieved by the Hartmann-Hahn transfer with optional mismatched condition on the ^{1}H channel.

potential benefit of high-resolution ^{13}C separated local-field experiments for OS NMR is hard to overestimate. With the availability of such SLF sequences a plethora of unexplored structural information is potentially obtainable from ^{13}C-derived structural restraints. The latter include $^{1}H_{\alpha}$-$^{13}C_{\alpha}$ dipolar couplings, which provide chiral restrictions [31–33] on the possible combinations of the torsion angles Φ_n and Ψ_n linking the ^{15}N-derived angular restraints for the adjacent peptide planes n and $n+1$ (cf. Fig. 1A). Moreover, the dipolar couplings arising from the beta and gamma carbons could be utilized for obtaining information about side chain conformations. Finally, by replacing or complementing the ^{15}N CSA with additional dipolar couplings measured per peptide plane (such as ^{15}N-^{13}C couplings) one can overcome uncertainties with regard to the tensor orientation and its principal values, which were shown to vary along the protein backbone [34–36]. The use of such "shiftless" angular restraints is expected to yield low-RMSD backbone structures for oriented membrane proteins [31]. Last but not least, the development of triple resonance ($^{1}H/^{13}C/^{15}N$) NMR experiments would put OS NMR on par with solution and MAS NMR, where such experiments have been successfully utilized for several decades.

Despite the above potential advantages, ^{13}C dimensions have not been widely employed in high-resolution OS NMR of membrane proteins with a few notable exceptions. For instance, Ishii and Tycko have proposed a ^{13}C-detected, ^{15}N -^{13}C correlation pulse sequence for spectroscopic assignment of uniformly doubly labeled samples [37]. A notable feature of this pulse sequence is that the ^{13}C signal is acquired under simultaneous homonuclear decoupling, which averages out the ^{13}C-^{13}C interactions over the sampling interval. Moreover, this technique has been extended to a three-dimensional experiment incorporating PISEMA [26] for the evolution of ^{1}H-^{15}N dipolar couplings, which directly provide structural information. Clearly, it would be of great advantage to be able to complement the ^{1}H-^{15}N DC's with ^{13}C-derived couplings such as ^{1}H-^{13}C and ^{13}C-^{15}N couplings. The angular-dependent ^{1}H-^{13}C dipolar couplings have been previously measured in macroscopically aligned samples include single crystals [38–41], bacteriophages [38,41], liquid crystals [42,43], and oriented lipid bicelles [44]. When the protein is expressed with selectively C_{α}-labeled aminoacids, good spectroscopic resolution can be obtained [38–40]. However, C_{α}-labeled precursors, in addition to being rather expensive, are currently commercially available for only a few types of aminoacids. When performed on uniformly of even partially labeled ^{13}C labeled samples, ^{13}C SLF NMR spectra typically exhibit insufficient spectroscopic resolution. Therefore, the most essential complication arising in this type of SLF experiments are the homonuclear ^{13}C-^{13}C dipolar interactions that are present in addition to the ^{1}H-^{1}H couplings in uniformly labeled samples; this issue gives rise to considerable theoretical challenges in developing high-resolution pulse sequences involving the evolution and detection of ^{1}H-^{13}C DC's.

Here we discuss some recent developments on triple-resonance ($^{1}H/^{13}C/^{15}N$) experiments performed on macroscopically aligned samples with emphasis on $^{1}H_{\alpha}$-$^{13}C_{\alpha}$ dipolar couplings detected at ^{15}N sites. Despite its inherently lower sensitivity than ^{13}C NMR, ^{15}N detection is advantageous in the sense that ^{15}N NMR generally exhibit narrower line widths than ^{13}C resonances due to the negligible ^{15}N-^{15}N dipolar couplings and a narrower CSA range for the amide nitrogen spins, thus allowing one to excite and evolve the entire ^{15}N NMR spectrum in the indirect spectroscopic dimension. Moreover, the common ^{15}N CSA dimension allows for direct juxtaposition of $^{1}H_{\alpha}$-$^{13}C_{\alpha}$ couplings onto its corresponding ^{1}H-^{15}N DCs for each of the amide resonances, which are obtainable from standard double-resonance SLF experiments. Furthermore, we report on preliminary developments on establishing intra- peptide vs. interpeptide ($^{13}C/^{15}N$) spin correlations using selective ^{15}N-filtering schemes and proton-mediated magnetization transfer between ^{13}C and ^{15}N spins under mismatched Hartmann-Hahn conditions on the ^{1}H channel. The developed family of pulse sequences are first illustrated on a^{15}N-labeled NAL crystal where ^{13}C NMR is performed at natural abundance and then extended to a uniformly doubly (^{15}N, ^{13}C) labeled sample of Pf1 coat protein reconstituted in magnetically aligned bicelles.

2. Prerequisites

2.1. Z-filtering with selective excitation

The relatively broad range for ^{13}C CSA (ranging from ca. 1–240 ppm, including the carbonyl regions) makes it difficult to optimally manipulate the entire spectroscopic region in two-dimensional (2D) ^{13}C spectra at moderate rf powers, which can give rise to improperly evolved peaks and spectral distortions at the zero- and Nyquist frequencies in the indirect (dipolar) dimension. Selective evolution of a target region in the NMR spectrum would greatly simplify its overall appearance and subsequent assignment. The idea of utilizing Gaussian pulses dates back to solution NMR experiments [45,46]. As was demonstrated a long time ago [45], the excitation profile of a Gaussian pulse has a sinc-like shape with alternating positive and negative intensities for the side excitation bands. It is possible to attenuate those artifacts by applying a truncation to the Gaussian pulse [46]. Application of such low rf-power Gaussian pulses can select a relatively narrow frequency region, thus simplifying the OS NMR spectra, as was demonstrated previously for ^{15}N SLF spectra [47]. Since the $^{1}H_{\alpha}$-$^{13}C_{\alpha}$ DCs are of primary interest here, as well as the ^{1}H-^{13}C dipole interactions arising from the carbon atoms forming side chains (such as C_{β} and C_{Υ} spin sites), a relatively narrow aliphatic region (30–80 ppm) can be excited using a selective z-filter incorporating a Gaussian pulse. Fig. 1b shows such a sequence for acquiring one-dimensional ^{13}C NMR spectra of selectively excited aliphatic regions. First, following cross-polarization, a soft 270-degree Gaussian pulse (truncated at 12%) is applied in the middle of the aliphatic region (ca. 50 ppm), which stores the ^{13}C spins resonating near this ppm range along the z-axis. Next, a short train of 4–5 saturating pulses can be optionally applied on the proton channel to avoid any Zeeman-to-Zeeman magnetization transfer to the ^{15}N spins (which may take place even under grossly mismatched Hartmann-Hahn conditions). Then the stored aliphatic carbon magnetization is brought back towards the x-axis for either direct ^{13}C detection (Fig. 1b) or subsequent proton-mediated transfer to ^{15}N spins and ^{15}N detection (cf. Fig. 1c and d) as discussed below.

2.2. Proton-mediated transfer under mismatched Hartmann-Hahn conditions

In addition to the widely employed spin-diffusion methods, an alternative way of establishing spin-spin correlations in the tilted rotating frame is based on the proton-mediated magnetization transfer under mismatched Hartmann-Hahn (MMHH) conditions [48]. Briefly, under the MMHH conditions the initial Zeeman order of energy of dilute spins is converted to the dipolar order of the bulk protons and then back to the Zeeman order, thereby establishing cross peaks. The MMHH technique, similarly to the TSAR technique in MAS [49], does not rely on the direct couplings between the dilute spins, and is generally applicable to both hetero- and homo-nuclear spin exchanges. As was demonstrated for the case of a single NAL crystal [48,50], correlations can be established for the ^{15}N spins separated by as far as 6.7 Å apart. The MMHH method is also suitable for spectroscopic assignment that involves establishing correlations between nearest neighbors, i.e. (n, $n\pm1$) spin sites, which are only 2.9 Å apart. Notably, the MMHH magnetization transfer occurs much more quickly (over a few ms) as compared to proton-driven spin diffusion, which typically requires several seconds for aligned samples. By using the MMHH pulse sequence, NMR assignments of Pf1 coat protein both expressed on the phage and reconstituted in magnetically aligned bicelles have been confirmed [51,52]. Recently, an automated algorithm has been developed for spectroscopic assignment of oriented membrane proteins utilizing the spin-exchange ^{1}H-^{15}N SLF and homonuclear ^{15}N-^{15}N correlation experiments [53]. A recent work by Lin and Opella [40] represents a clever extension of the MMHH method to triple-resonance experiments, which allow one to correlate ^{15}N and ^{13}C spin-bearing nuclei in oriented samples. Despite these significant advances, however, assignment challenges remain, which are mainly

associated with peak crowding and the relatively weak cross-peak intensities. This also emphasizes the necessity of developing triple-resonance techniques for OS NMR to improve spectroscopic resolution by introducing additional dimensions.

2.3. The ROULETTE family of pulse sequences

A family of computer generated windowless pulse sequences (PS's) for evolving ^{1}H-^{15}N and ^{1}H-^{13}C dipolar couplings have been recently reported [54,55]. The method of generating such sequences *in silico* has been termed ROULETTE – Random Optimization Using the Liouville Equation Tailored To the Experiment. It was shown that highly efficient PS's can be generated without the use of Average Hamiltonian Theory by solving numerically the many-body Liouville-von Neumann equation. The resulting sequences are screened against a cumulative target function in the frequency domain, which scores the PS candidates for the correctly evolved dipolar coupling frequencies and their linewidths. The target function is minimized using an adaptive-temperature Monte-Carlo simulated annealing protocol while searching over an extensive parameter range involving non-quadrature phases, arbitrary pulse durations, and power application schemes. The ROULETTE blocks shown in Fig. 1C and D consist of a generic 6-subdwell windowless architecture with pulse phases φ_{ij}, ψ_{ij} and durations t_j . The phases for the even and odd dwells (denoted by φ and ψ, respectively) in general can have distinct values. Additional symmetry and antisymmetry conditions are imposed for the pulse durations and phases, i.e.$\varphi_{i,j} = \overline{\varphi}_{i,N-j+1}$ and $\psi_{i,j} = \overline{\psi}_{i,N-j+1}$(for $N = 6$ subdwells, with bar denoting a 180-degree phase shift) [54,55].

The full possible range of the ^{1}H-^{13}C dipolar couplings of ca. +/- 23 kHz necessitates the use of pulse sequences having either shorter dwell times and/or smaller scaling factors. This is necessary so that these PS's would be applicable to lossy biological samples, where the total dwell time inversely scales with the amplitudes of the rf B_1 fields generated by the NMR probe, which typically do not exceed 50–60 kHz. For instance, at an rf field strength of $\nu_{rf} = 50$ kHz yielding the 90° pulse time $t_{90} = 5$ μs neither PISEMA nor SAMPI4 would be able to fully cover this range since their Nyquist frequencies in the dipolar dimension would be $1/(32 \times t_{90}/3) = 18.8$ kHz and just $1/(16 \times t_{90} \times 1.0927) = 11.4$ kHz, respectively. By contrast, the ROULETTE-CAHA sequence spans the frequencies up to +/-27.2 kHz at $\nu_{rf} = 50$ kHz [55], which is sufficient to cover the entire spectroscopic range required for the evolution of ^{1}H-^{13}C dipolar couplings at this moderate rf amplitude.

The ROULETTE-based 2D pulse sequences used in this work are outlined in Fig. 1C and D. The sequences are entirely windowless and all pulses are applied on resonance. The phase and duration parameters for the two ν_{rf} nutation frequencies of 50 and 63 kHz used to evolve ^{1}H-^{13}C dipolar couplings are given in Table 1. The scaling factor was determined numerically at 0.58 [55]. It can be seen that the phases are similar at the two rf nutation frequencies while the pulse durations are generally longer at smaller nutation frequencies. Also listed in Table 1 are the parameters for the ROULETTE 2.0 sequence used to measure the ^{1}H-^{15}N dipolar coupling with the theoretical scaling factor of 0.725 [55]. While the original ROULETTE 2.0 sequence was optimized for $\nu_{\mathrm{rf}} = 58$ kHz, the timings in Table 1 were simply rescaled to make them proportionally longer in order to correspond to the experimentally determined nutation frequency of 48 kHz for the Pf1 sample (see below). Fig. 1C depicts a double-resonance PS, where the ROULETTE block is used to evolve ^{1}H-^{13}C couplings in the t_1 dimension and the ^{15}N decoupling can be optionally applied during the ^{13}C detection (t_2 dimension). Fig. 1D shows a triple-resonance pulse sequence where the evolved ^{1}H-^{13}C dipolar couplings are filtered through and detected at the ^{15}N amide sites. Here the magnetization transfer from ^{13}C to ^{15}N spins is implemented using either direct ^{13}C-^{15}N Hartmann-Hahn transfer (i.e. when no irradiation on the proton channel is applied), or via proton-mediated transfer under the MMHH conditions when the proton channel is irradiated at slightly (about 5 kHz) above the matching condition. Both pulse sequences utilize a Gaussian z-filter to reduce the magnetization arising from the carbonyl and methyl carbons, which exhibit much smaller and broader dipolar couplings that convey little useful structural information.

3. Experimental

All experiments have been performed using a 5 mm solenoid E-free triple-resonance Bruker probe and a 500 MHz ^{1}H frequency Bruker Avance II spectrometer. The Pf1 bicelle sample containing ca. 4 mg of the uniformly (^{15}N, ^{13}C) labeled protein was prepared as previously described [56], by using isotopically labeled ^{15}N ammonium chloride and ^{13}C glucose as the ^{15}N and ^{13}C precursors, respectively. For the ^{15}N-labeled NAL crystal sample (18 mg), to evolve ^{1}H-^{13}C DC's the 90-degree pulse was calibrated at 4.07 μs, 128/256 scans were acquired for the ^{15}N decoupled/coupled ^{13}C-detected experiments, respectively, for each of the 128 t_1 points. For the biological sample of Pf1 coat protein, the 90-degree pulse was calibrated at 5.2 μs and the spectra were measured at 37 °C. For ^{15}N-detected triple-resonance experiments 2048 scans were acquired for both ^{15}N labeled, ^{13}C natural-abundance NAL crystal and uniformly (^{15}N, ^{13}C) labeled Pf1 coat protein. Due to the low signal-to-noise ratios and longer acquisition times ca. 40 t_1 points were typically acquired in the 2D triple-resonance experiments. The MMHH transfer was performed at ca. $\nu_{rf} = 30$ kHz for ^{13}C and ^{15}N, and at ca. 35 kHz for ^{1}H. The length of the 12%-truncated 270-degree Gaussian pulse was set to 350 μs and the power level was calibrated to achieve the optimal selectivity for the aliphatic ^{13}C region at around 50 ppm. The MMHH contact time was 2.4 ms for NAL and 3 ms for the Pf1 coat protein sample, respectively. The ROULETTE 2.0 sequence was run on the Pf1 sample with 128 scans per each of the 128 t_1 points. Heteronuclear decoupling of the ^{1}H, ^{13}C, or ^{15}N spins during the acquisitions (t_2 domain) was achieved using the SPINAL-16 sequence [57]. Data were processed using nmrPipe [58].

4. Results

The spectra acquired using the sequence of Fig. 1B are shown in Fig. 2. The positive intensity is equivalent to applying a hard 90-degree pulse before the z-filter and the negative intensity corresponds to the mostly aliphatic region filtered out by a soft Gaussian 270-degree pulse applied before the z-filter with the ^{13}C NMR carrier frequency centered at ca. 50 ppm. As can be seen, the application of selective Gaussian pulse allows one to greatly reduce the intensities of the less informative carbonyl and methyl peak regions. The *z*-filter thus selects mostly the aliphatic ^{1}H-^{13}C dipolar couplings that are subsequently transferred to the ^{15}N spin sites in the two dimensional experiments as described above.

Fig. 3A shows ^{15}N-coupled, ^{13}C -detected SLF spectrum obtained using the sequence of Fig. 1C incorporating the ROULETTE-CAHA PS in the indirect dimension. The dipolar resonances arising from the $^{13}C_{\alpha}$ sites are easily identifiable by the presence of doublets in the direct dimension

Table 1
The pulse parameters for ROULETTE-CAHA sequence optimized at $\nu_{rf} = 50$ kHz and 63 kHz and ROULETTE 2.0 sequence for measuring ^{1}H-^{15}N dipolar couplings with subdwell timings rescaled to $\nu_{rf} = 48$ kHz.

Sequence	φ_{11}	φ_{12}	φ_{13}	φ_{21}	φ_{22}	φ_{23}	ψ_{11}	ψ_{12}	ψ_{13}	ψ_{21}	ψ_{22}	ψ_{23}	t_1(μs)	t_2(μs)	t_3(μs)
ROULETTE-CAHA at 50 kHz	229.1	159.9	180.8	229.0	154.5	201.2	65.7	359.6	251.0	283.2	7.0	241.0	7.81	6.59	1.26
ROULETTE-CAHA at 63 kHz	234.7	159.4	257.9	228.1	155.3	197.8	65.1	5.4	287.5	285.5	7.4	185.8	6.48	5.15	2.16
ROULETTE-2.0 at 48 kHz	201.5	189.6	141.3	247.5	288.1	181.9	176.4	151.9	272.5	153.8	165.3	72.7	13.59	3.94	7.99

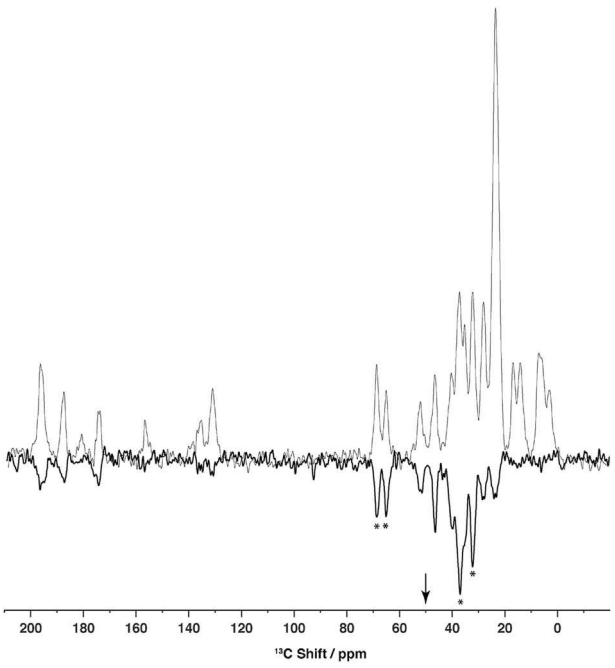

Fig. 2. Superposition of the fully excited ^{13}C (positive intensity) and selectively filtered (negative intensity) spectra of ^{15}N labeled NAL single crystal measured at ^{13}C natural abundance using the pulse sequence of Fig. 1B. The selective 270-degree Gaussian pulse before the *z*-filter allows one to attenuate the structurally less informative carbonyl and methyl regions. The resonances arising from the $^{13}C_\alpha$ carbons of interest are marked with asterisks and the position of the carrier frequency at 50 ppm is marked by an arrow.

due to their interactions with the directly bonded ^{15}N amide spins. Due to the presence of four (4) distinct molecular orientations in the unit cell for the NAL crystal, 4x2 = 8 $^{13}C_\alpha$ resonances are observed. A slice through the peak at 9 kHz in the vertical dimension shows the smallest observed $^{13}C\alpha$-^{15}N coupling. Fig. 3B shows an ^{15}N-detected 2D spectrum using the pulse sequence of Fig. 1D acquired with ^{13}C decoupling applied during the ^{15}N acquisition. Direct Hartmann Hahn transfer from ^{13}C to ^{15}N spins was utilized in this case with the ^{1}H rf power turned off. Almost exclusively intrapeptide $C_\alpha H_\alpha$ couplings are transferred from the directly bonded $^{13}C_\alpha$ spins to the ^{15}N sides, which necessitates the use of ^{13}C decoupling. Without the ^{13}C decoupling during the acquisition the peaks would become split in the ^{15}N dimension (not shown). We also note that the relative intensities of the $C_\alpha H_\alpha$ peaks in Fig. 3B are commensurate with the magnitudes of the $^{13}C_\alpha$-^{15}N couplings observed in Fig. 3A, which require different mixing times to achieve the maximum possible transfer intensity.

Fig. 4A shows ^{13}C-detected SLF spectrum obtained using the same ROULETTE-CAHA sequence, albeit with ^{15}N decoupling during the acquisition, cf. Fig. 1C. The full spectral range is shown to depict all resolved ^{1}H-^{13}C resonances including the carbonyl and methyl regions. In addition, as compared to Fig. 3A, single peaks are now observed for the four C_α sites due to the application of ^{15}N decoupling. Fig. 4B shows ^{15}N-detected spectrum using the pulse sequence of Fig. 1D, albeit without ^{13}C decoupling. Proton-mediated MMHH transfer was utilized in this case with ^{1}H rf power being ca. 5 kHz above the matching condition. Most if not all dipolar ^{1}H-^{13}C couplings observed in Fig. 4A between 20 and 80 ppm are now transferred to the ^{15}N sites. Interestingly, no additional splittings are observed in the ^{15}N dimension even though ^{13}C decoupling was not applied, which points to a predominantly long-distance or intermolecular nature of the correlations. A simple estimate shows that for a single cross peak to occur at natural ^{13}C abundance, an intermolecular magnetization transfer would need to originate approximately from one out of 12 nearby molecules (having 8 carbons each). The surrounding NAL molecules are separated by 6–7 Å from each other in the crystal lattice, which provides an approximate lower limit for the distance of such a transfer. Thus, statistically it is 100 times more probable to have at least one surrounding NAL molecule with a ^{13}C carbon than having a $^{13}C_\alpha$ carbon next to an ^{15}N amide spin, which explains the predominantly intermolecular nature of the dipolar cross peaks.

As an extension of the presented pulse sequences to biological samples, Fig. 5 depicts ^{15}N-detected SLF spectra of Pf1 coat protein reconstituted in magnetically aligned bicelles. Fig. 5A shows a triple-resonance ^{1}H-^{13}C SLF spectrum detected at ^{15}N sites [33] acquired using the ROULETTE-CAHA sequence in the indirect dimension. The resolution in Fig. 5A appears to be somewhat better than in the spectrum of ref. [33] which was acquired by applying a double SAMPI4 sequence on ^{13}C and ^{1}H channels to evolve the ^{1}H-^{13}C dipolar couplings. Spectroscopic assignments for the ^{1}H-^{13}C peaks corresponding to those from Ref. [33] are also given in Fig. 5A. Additional peaks can be seen, which may be due to a transfer from nearby carbonyl atoms and long-distance transfer from the side-chain carbons. Further experiments are needed to delineate between these multiple (per ^{15}N site) dipolar peaks arising in the ^{1}H-^{13}C/^{15}N SLF spectrum of Fig. 5A. It should also be noted that the triple-resonance spectrum of Fig. 5A was obtained at the limit of sensitivity afforded by the 500 MHz ^{1}H frequency spectrometer requiring as many as 2k scans per t_1 point yielding just ca. 5:1 signal-to-noise ratio; whereas the spectrum reported in Ref. [33] has been averaged by co-adding four (4) separate spectra to increase sensitivity. Fig. 5B shows the "traditional" two-dimensional ^{1}H-^{15}N SLF spectrum obtained with ROULETTE 2.0 which can help establish assignments for the $^{1}H_\alpha$ -$^{13}C_\alpha$ peaks. ^{13}C

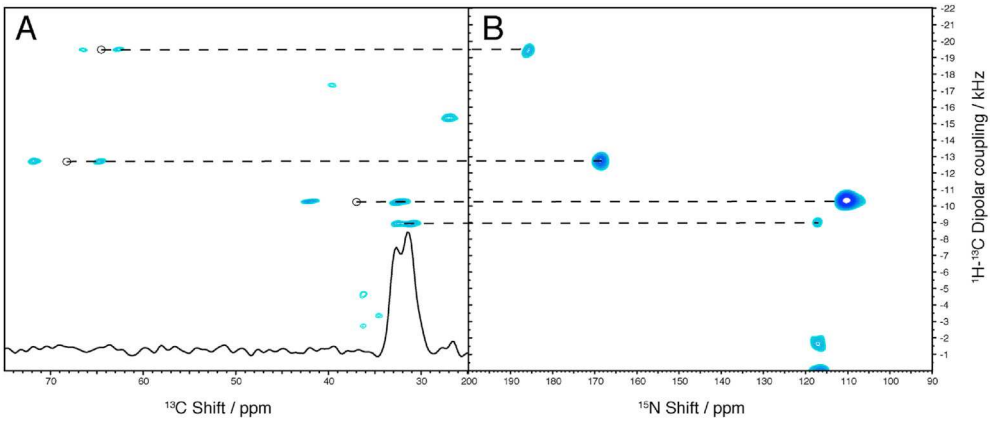

Fig. 3. A. NAL spectrum acquired with the ^{13}C-detected pulse sequence of Fig. 1C without ^{15}N decoupling during the acquisition. The $^{1}H_\alpha$ -$^{13}C_\alpha$ peaks are identifiable by the presence of additional splittings in the ^{13}C dimension. B. ^{15}N-detected sequence of Fig. 1D with ^{13}C decoupling exhibiting four (4) $^{1}H_\alpha$ -$^{13}C_\alpha$ intramolecular peaks with the dipolar frequencies matching those of part A are shown by dashed lines.

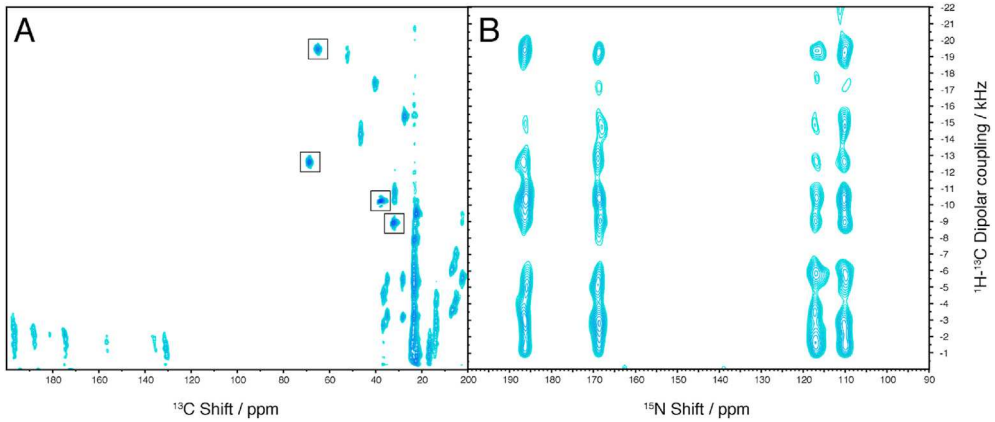

Fig. 4. A. ^{13}C-detected pulse sequence of Fig. 1C with ^{15}N decoupling applied during the acquisition. Full spectral range in the ^{13}C dimension is shown. The dipolar resonances arising from $^{13}C_{\alpha}$ spins are outlined by squares. B. The sequence of Fig. 1D evolves multiple $^{1}H_{\alpha}$ -$^{13}C_{\alpha}$ distant intermolecular peaks detected at ^{15}N sites, which does not require ^{13}C decoupling due to the distant nature of the magnetization transfer.

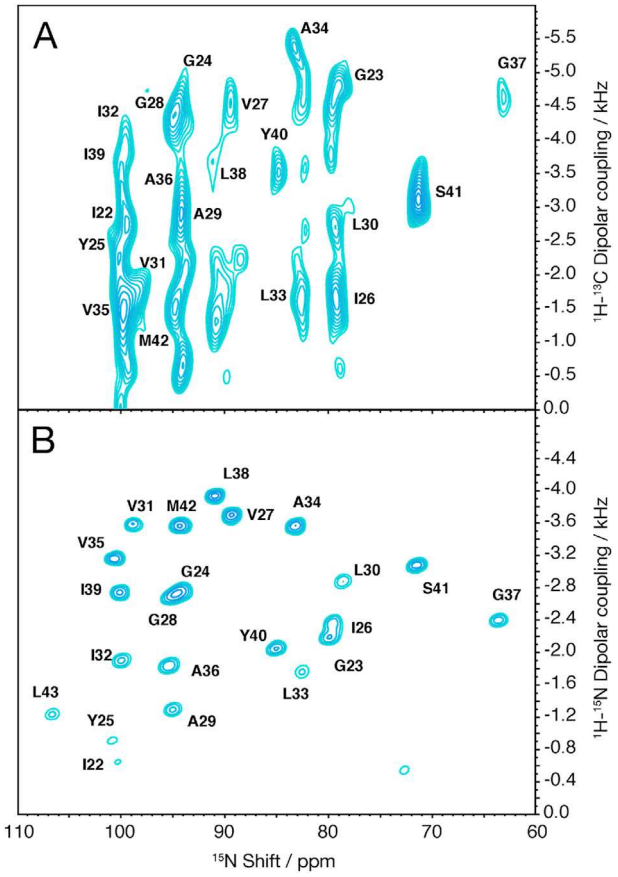

Fig. 5. Triple-resonance SLF spectra for uniformly, doubly (^{13}C, ^{15}N) labeled Pf1 coat protein reconstituted in magnetically aligned bicelles. A. $^{1}H_{\alpha}$ -$^{13}C_{\alpha}$ dipolar couplings evolved using ROULETTE-CAHA pulse sequence and detected at ^{15}N sites using PS of Fig. 2D. B. ^{1}H-^{15}N/^{15}N SLF experiment based on ROULETTE 2.0 with ^{13}C decoupling applied during the ^{15}N acquisition. Direct juxtaposition allows one to correlate ^{1}H-^{15}N and $^{1}H_{\alpha}$ -$^{13}C_{\alpha}$ couplings for each aminoacid within the transmembrane region. Additional peaks (per ^{15}N resonance) can also be seen in part A, presumably arising from the carbonyl carbons and other aliphatic regions. Of note is excellent resolution in the ^{1}H-^{15}N dipolar dimension and peak uniformity observed in part B.

decoupling has been applied during the ^{15}N CSA evolution in both spectra. Excellent resolution is seen in Fig. 5B exhibiting dipolar linewidths in the range of 120–170 Hz. This is to be compared with the

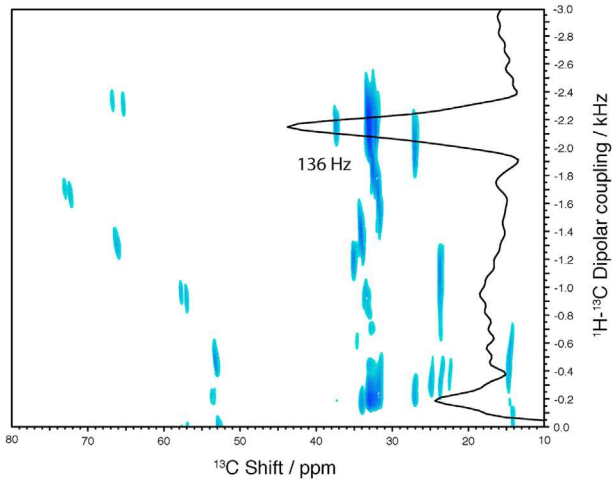

Fig. 6. Double-resonance ^{1}H-^{13}C/^{13}C SLF spectrum of magnetically aligned DMPC/DHPC bicelles acquired using the ROULETTE-CAHA sequence at natural ^{13}C abundance. A representative slice through the dipolar dimension is shown to illustrate the linewidths obtained with this pulse sequence.

typical linewidths in the dipolar dimension obtainable with either PISEMA or SAMPI4 PS, which are typically around 200 Hz. Importantly, due to the ^{13}C decoupling, the spectrum for the doubly labeled sample looks just as a singly labeled ^{15}N spectrum without compromising resolution. These spectra demonstrate that the ROULETTE family of pulse sequences developed *in silico* and tested on NAL crystal are directly applicable to biological samples.

Finally, the two-dimensional ROULETTE-CAHA sequence could be useful for NMR studies of the structure and dynamics of magnetically aligned liquid crystals [42,43], and oriented lipid bicelle bilayers [44]. Shown in Fig. 6 is the ROULETTE-CAHA SLF spectrum of blank DMPC/DHPC bicelles acquired at natural ^{13}C abundance, which is to be compared with the spectrum reported in Refs. [44]. Here, 256 scans have been averaged for each of the 96 t_1 points. The linewidths recorded in the ^{1}H-^{13}C dipolar dimension are generally less than 200 Hz, with the best linewidth being as narrow as about 130 Hz. Such a high resolution is especially advantageous for probing the relatively narrow dipolar coupling range (<2.4 kHz), which arises due to the dynamic averaging of the ^{1}H-^{13}C spin-spin couplings by the lipid motions.

5. Conclusions

Further advancement of OS NMR of membrane proteins will greatly

benefit from the development of new triple-resonance experiments for spectroscopic assignment and obtaining additional angular restraints. Incorporation of ^{13}C-derived restraints is expected to greatly improve the convergence of structures calculated from OS NMR which would extend this technique to structure determination of protein backbone segments of arbitrary topology, as well as side chains. We have summarized ongoing developments of a new family of high-resolution triple-resonance (^{1}H/^{13}C/^{15}N) pulse sequences that can be utilized to probe the chiral $^{1}H_{\alpha}$-$^{13}C_{\alpha}$ dipolar couplings transferred to the ^{15}N amide spin sites. Moreover, the filtering of the ^{1}H-^{13}C dipolar couplings through amide ^{15}N amide spins increases spectroscopic resolution. While the results presented here contain two-dimensional experiments performed at a relatively moderate ^{1}H frequency of 500 MHz, future extensions of these sequences to three-dimensional experiments, which would only be feasible at higher magnetic fields, appear to be relatively straightforward. Finally, we note that if sufficient signal-to-noise ratios could be achieved, experiments performed at complete ^{15}N labeling and ^{13}C natural abundance might be informative with regard to probing intermolecular vs. intramolecular and short-range vs. long-range spin correlations in comparison with uniformly doubly labeled samples where the intramolecular interactions are predominant.

Declaration of competing interest

The authors declare that they have no known competing financial interests or personal relationships that could have appeared to influence the work reported in this paper.

Acknowledgements

This material is based upon work supported by the National Science Foundation under Grant No. MCB 1818240 and by the U.S. Army Research Office under contract number W911NF1810363.

References

[1] P.A. McDonnell, K. Shon, Y. Kim, S.J. Opella, Fd coat protein structure in membrane environments, J. Mol. Biol. 233 (1993) 447–463.
[2] S.J. Opella, F.M. Marassi, J.J. Gesell, A.P. Valente, Y. Kim, M. Oblatt-Montal, M. Montal, Structures of the M2 channel-lining segments from nicotinic acetylcholine and NMDA receptors by NMR spectroscopy, Nat. Struct. Biol. 6 (1999) 374–379.
[3] J. Wang, S. Kim, F. Kovacs, T.A. Cross, Structure of the transmembrane region of the M2 protein H+ channel, Prot. Sci. 10 (2001) 2241–2250.
[4] F.M. Marassi, S.J. Opella, Simultaneous assignment and structure determination of a membrane protein from NMR orientational restraints, Prot. Sci. 12 (2003) 403–411.
[5] N.J. Traaseth, J.J. Buffy, J. Zamoon, G. Veglia, Structural dynamics and topology of phospholamban in oriented lipid bilayers using multidimensional solid-state NMR, Biochemistry 45 (2006) 13827–13834.
[6] N.J. Traaseth, K.N. Ha, R. Verardi, L. Shi, J.J. Buffy, L.R. Masterson, G. Veglia, Structural and dynamic basis of phospholamban and sarcolipin inhibition of Ca2+-ATPaset, Biochemistry 47 (2008) 3–13.
[7] N.J. Traaseth, L. Shi, R. Verardi, D.G. Mullen, G. Barany, G. Veglia, Structure and topology of monomeric phospholamban in lipid membranes determined by a hybrid solution and solid-state NMR approach, Proc. Natl. Acad. Sci. U. S. A. 106 (2009) 10165–10170.
[8] R. Verardi, L. Shi, N.J. Traaseth, N. Walsh, G. Veglia, Structural topology of phospholamban pentamer in lipid bilayers by a hybrid solution and solid-state NMR method, Proc. Natl. Acad. Sci. U. S. A. 108 (2011) 9101–9106.
[9] K. Yamamoto, M. Gildenberg, S. Ahuja, S.C. Im, P. Pearcy, L. Waskell, A. Ramamoorthy, Probing the transmembrane structure and topology of microsomal cytochrome-P450 by solid-state NMR on temperature-resistant bicelles, Sci. Rep. 3 (2013) 2556.
[10] N.J. Gleason, V.V. Vostrikov, D.V. Greathouse, R.E. Koeppe, Buried lysine, but not arginine, titrates and alters transmembrane helix tilt, Proc. Natl. Acad. Sci. U. S. A. 110 (2013) 1692–1695.
[11] M. Sharma, M.G. Yi, H. Dong, H.J. Qin, E. Peterson, D.D. Busath, H.X. Zhou, T.A. Cross, Insight into the mechanism of the influenza A proton channel from a structure in a lipid bilayer, Science 330 (2010) 509–512.
[12] C.R. Sanders, J.H. Prestegard, Magnetically orientable phospholipid bilayers containing small amounts of a bile salt analogue, CHAPSO, Biophys. J. 58 (1990) 447–460.
[13] C.R. Sanders, J.P. Schwonek, Characterization of magnetically orientable bilayers in mixtures of DHPC and DMPC by solid state NMR, Biochem 31 (1992) 8898–8905.
[14] R.R. Vold, R.S. Prosser, Magnetically oriented phospholipid bilayered micelles for structural studies of polypeptides. Does the ideal bicelle exist? J. Magn. Reson. B 113 (1996) 267–271.
[15] K.J. Glover, J.A. Whiles, G. Wu, N.-J. Yu, R. Deems, J.O. Struppe, R.E. Stark, E.A. Komives, R.R. Vold, Structural evaluation of phospholipid bicelles for solution-state studies of membrane-associated biomolecules, Biophys. J. 81 (2001) 2163–2171.
[16] U.H.N. Durr, M. Gildenberg, A. Ramamoorthy, The magic of bicelles lights up membrane protein structure, Chem. Rev. 112 (2012) 6054–6074.
[17] A. Gayen, J.R. Banigan, N.J. Traaseth, Ligand-induced conformational changes of the multidrug resistance transporter EmrE probed by oriented solid-state NMR spectroscopy, Angew. Chem. Int. Ed. 52 (2013) 10321–10324.
[18] F. Scholz, E. Boroske, W. Helfrich, Magnetic-anisotropy of lecithin membranes - a new anisotropy susceptometer, Biophys. J. 45 (1984) 589–592.
[19] R.S. Prosser, J.S. Hwang, R.R. Vold, Magnetically aligned phospholipid bilayers with positive ordering: a new model membrane system, Biophys. J. 74 (1998) 2405–2418.
[20] R. Verardi, N.J. Traaseth, L. Shi, F. Porcelli, L. Monfregola, S. De Luca, P. Amodeo, G. Veglia, A. Scaloni, Probing membrane topology of the antimicrobial peptide distinctin by solid-state NMR spectroscopy in zwitterionic and charged lipid bilayers, Biochim. Biophys. Acta Biomembr. 1808 (2011) 34–40.
[21] S.H. Park, C. Loudet, F.M. Marassi, E.J. Dufourc, S.J. Opella, Solid-state NMR spectroscopy of a membrane protein in biphenyl phospholipid bicelles with the bilayer normal parallel to the magnetic field, J. Magn. Reson. 193 (2008) 133–138.
[22] S.H. Park, S. Berkamp, G.A. Cook, M.K. Chan, H. Viadiu, S.J. Opella, Nanodiscs versus macrodiscs for NMR of membrane proteins, Biochemistry 50 (2011) 8983–8985.
[23] T. Ravula, S.K. Ramadugu, G. Di Mauro, A. Ramamoorthy, Bioinspired, size-tunable self-assembly of polymer-lipid bilayer nanodiscs, Angew. Chem. Int. Ed. 56 (2017) 11466–11470.
[24] J. Radoicic, S.H. Park, S.J. Opella, Macrodiscs comprising SMALPs for oriented sample solid-state NMR spectroscopy of membrane proteins, Biophys. J. 115 (2018) 22–25.
[25] S.H. Park, J. Wu, Y. Yao, C. Singh, Y. Tian, F.M. Marassi, S.J. Opella, Membrane proteins in magnetically aligned phospholipid polymer discs for solid-state NMR spectroscopy, Biochim. Biophys. Acta Biomembr. 1862 (2020) 183333.
[26] C.H. Wu, A. Ramamoorthy, S.J. Opella, High-resolution heteronuclear dipolar solid-state NMR spectroscopy, J. Magn. Reson. A 109 (1994) 270–272.
[27] S.V. Dvinskikh, K. Yamamoto, A. Ramamoorthy, Heteronuclear isotopic mixing separted local field NMR spectroscopy, J. Chem. Phys. 125 (2006), 034507.
[28] A.A. Nevzorov, S.J. Opella, Selective averaging for high-resolution solid-state NMR spectroscopy of aligned samples, J. Magn. Reson. 185 (2007) 59–70.
[29] P.L. Stewart, R. Tycko, S.J. Opella, Peptide backbone conformation by solid-state nuclear magnetic resonance spectroscopy, J. Chem. Soc. Faraday Trans. I 84 (1988) 3803–3819.
[30] R. Bertram, T. Asbury, F. Fabiola, J.R. Quine, T.A. Cross, M.S. Chapman, Atomic refinement with correlated solid-state NMR restraints, J. Magn. Reson. 163 (2003) 300–309.
[31] Y.Y. Yin, A.A. Nevzorov, Structure determination in "shiftless" solid state NMR of oriented protein samples, J. Magn. Reson. 212 (2011) 64–73.
[32] J. Lapin, A.A. Nevzorov, Validation of protein backbone structures calculated from NMR angular restraints using Rosetta, J. Biomol. NMR 73 (2019) 229–244.
[33] E.O. Awosanya, J. Lapin, A. Nevzorov, NMR" crystallography" for uniformly (13C, 15N) labeled oriented membrane proteins, Angew Chem. Int. Ed. Engl. 132 (2020) 3582–3585.
[34] G. Cornilescu, A. Bax, Measurement of proton, nitrogen, and carbonyl shielding anisotropies in a protein dissolved in a dilute liquid crystalline phase, J. Am. Chem. Soc. 122 (2000) 10143–10154.
[35] J.R. Brender, D.M. Taylor, A. Ramamoorthy, Orientation of amide nitrogen-15 chemical shift tensor in peptides: a quantum chemical study, J. Am. Chem. Soc. 123 (2001) 914–922.
[36] S. Paramasivam, A.M. Gronenborn, T. Polenova, Backbone amide N-15 chemical shift tensors report on hydrogen bonding interactions in proteins: a magic angle spinning NMR study, Solid State Nucl. Magn. Reson. 92 (2018) 1–6.
[37] Y. Ishii, R. Tycko, Multidimensional heteronuclear correlation spectroscopy of a uniformly 15N- and 13C-labeled peptide crystal: toward spectral resolution, assignment, and structure determination of oriented molecules in solid-state NMR, J. Am. Chem. Soc. 122 (2000) 1443–1455.
[38] N. Sinha, C.V. Grant, S.H. Park, J.M. Brown, S.J. Opella, Triple resonance experiments for aligned sample solid-state NMR of C-13 and N-15 labeled proteins, J. Magn. Reson. 186 (2007) 51–64.
[39] E.C. Lin, C.H. Wu, Y.A. Yang, C.V. Grant, S.J. Opella, H-1-C-13 separated local field spectroscopy of uniformly C-13 labeled peptides and proteins, J. Magn. Reson. 206 (2010) 105–111.
[40] E.C. Lin, S.J. Opella, H-1 assisted C-13/N-15 heteronuclear correlation spectroscopy in oriented sample solid-state NMR of single crystal and magnetically aligned samples, J. Magn. Reson. 211 (2011) 37–44.
[41] B.B. Das, E.C. Lin, S.J. Opella, Experiments optimized for magic angle spinning and oriented sample solid-state NMR of proteins, J. Phys. Chem. B 117 (2013) 12422–12431.
[42] M.K. Reddy, K.S. Reddy, T. Narasimhaswamy, B.B. Das, N.P. Lobo, K.V. Ramanathan, C-13-H-1 dipolar couplings for probing rod-like hydrogen bonded mesogens, New J. Chem. 37 (2013) 3195–3206.
[43] M.K. Reddy, E. Varathan, N.P. Lobo, A. Roy, T. Narasimhaswamy, K.V. Ramanathan, Mono layer to interdigitated partial bilayer smectic C transition

in thiophene-based spacer mesogens: X-ray diffraction and C-13 nuclear magnetic resonance studies, Langmuir 31 (2015) 10831–10842.
[44] S.V. Dvinskikh, U.H. Durr, K. Yamamoto, A. Ramamoorthy, High-resolution 2D NMR spectroscopy of bicelles to measure the membrane interaction of ligands, J. Am. Chem. Soc. 129 (2007) 794–802.
[45] C. Bauer, R. Freeman, T. Frenkiel, J. Keeler, A.J. Shaka, Gaussian pulses, J. Magn. Reson. 58 (1984) 442–457.
[46] S. Davies, J. Friedrich, R. Freeman, Two-dimensional spectroscopy without an evolution period-"pseudo-COSY", J. Magn. Reson. 75 (1987) 540–545.
[47] S.N. Koroloff, A.A. Nevzorov, Selective excitation for spectral editing and assignment in separated local field experiments of oriented membrane proteins, J. Magn. Reson. 274 (2017) 7–12.
[48] A.A. Nevzorov, Mismatched hartmann-hahn conditions cause proton-mediated intermolecular magnetization transfer between dilute low spin nuclei in NMR of static solids, J. Am. Chem. Soc. 130 (2008) 11282–11283.
[49] J.R. Lewandowski, G. De Paepe, R.G. Griffin, Proton assisted insensitive nuclei cross polarization, J. Am. Chem. Soc. 129 (2007) 728–729.
[50] A.A. Nevzorov, High-resolution local-field spectroscopy with internuclear correlations, J. Magn. Reson. 201 (2009) 111–114.
[51] R.W. Knox, G.J. Lu, S.J. Opella, A.A. Nevzorov, A resonance assignment method for oriented-sample solid-state NMR of proteins, J. Am. Chem. Soc. 132 (2010) 8255–8257.
[52] W.X. Tang, R.W. Knox, A.A. Nevzorov, A spectroscopic assignment technique for membrane proteins reconstituted in magnetically aligned bicelles, J. Biomol. NMR 54 (2012) 307–316.
[53] J. Lapin, A.A. Nevzorov, Automated assignment of NMR spectra of macroscopically oriented proteins using simulated annealing, J. Magn. Reson. 293 (2018) 104–114.
[54] J. Lapin, A.A. Nevzorov, De novo NMR pulse sequence design using Monte-Carlo optimization techniques, J. Magn. Reson. 310 (2020) 106641.
[55] J. Lapin, A.A. Nevzorov, Computer-Generated pulse sequences for 1H-15N and 1Hα-13Cα Separated local-field experiments, J. Magn. Reson. (2020) 106794.
[56] S.H. Park, F.M. Marassi, D. Black, S.J. Opella, Structure and dynamics of the membrane-bound form of Pf1 coat protein: implications of structural rearrangement for virus assembly, Biophys. J. 99 (2010) 1465–1474.
[57] B.M. Fung, A.K. Khitrin, K. Ermolaev, An improved broadband decoupling sequence for liquid crystals and solids, J. Magn. Reson. 142 (2000) 97–101.
[58] F. Delaglio, S. Grzesiek, G.W. Vuister, G. Zhu, J. Pfeifer, A. Bax, NMRPipe: a multidimensional spectral processing system based on UNIX pipes, J. Biomol. NMR 6 (1995) 277–293.